Injectable shear-thinning hydrogels engineered with a self-assembling Dock-and-Lock mechanism

Hoang D. Lu, Manoj B. Charati, Iris L. Kim, Jason A. Burdick*

Department of Bioengineering, University of Pennsylvania, Philadelphia, PA, USA

ABSTRACT

Injected therapeutics, such as cells or biological molecules, may have enhanced efficiency when delivered within a scaffold carrier. Here, we describe a dual-component Dock-and-Lock (DnL) self-assembly mechanism that can be used to construct shear-thinning, self-healing, and injectable hydrogels. One component is derived from the RIIα subunit of cAMP-dependent kinase A and is engineered as a telechelic protein with end groups that dimerize (docking step). The second component is derived from the anchoring domain of A-kinase anchoring protein (AD) and is attached to multi-arm crosslinker polymers and binds to the docked proteins (locking step). When mixed, these two DnL components form robust physical hydrogels instantaneously and under physiological conditions. Mechanical properties and erosion rates of DnL gels can be tuned through the AD peptide sequence, the concentration and ratio of each component, and the number of peptides on the cross-linking polymer. DnL gels immediately self-recover after deformation, are resistant to yield at strains as high as 400%, and completely self-heal irrespective of prior mechanical disruption. Mesenchymal stem cells mixed in DnL gels and injected through a fine needle remain highly viable (>90%) during the encapsulation and delivery process, and encapsulated large molecules are released with profiles that correspond to gel erosion. Thus, we have used molecular engineering strategies to develop cytocompatible and injectable hydrogels that have the potential to support cell and drug therapies.

© 2011 Elsevier Ltd. All rights reserved.

1. Introduction

Hydrogels are water-swollen polymer networks and may be used to improve the efficiency of encapsulated therapeutics in cell and drug delivery applications, by controlling the release and retention of the therapeutic at the desired location [1]. Injectable hydrogels hold particular biomedical value because they may be implanted into tissues with minimally invasive methods and can accommodate irregularly shaped defects [2–4]. Hydrogel precursors are typically injected in liquid form and cross-linked *in situ* by chemical linkers, enzymes, photoinitiated polymerization, or by shifts in pH, temperature, and ionic strength [5–8]. However, cells and drugs delivered with these methods may be detrimentally affected by exposure to toxic reagents and non-physiological conditions [9]. Additionally, systems with slow gelation kinetics may suffer from significant cargo loss and diffusion from the target site, and exceedingly rapid gelation kinetics may result in premature polymerization and delivery failure [10,11].

Shear-thinning and self-healing hydrogels that flow and deform into liquids when under shear-stress and recover back into hydrogels when stress is removed are a promising class of materials for use as cell and drug carriers [12,13]. Cargo may be homogenously encapsulated *ex vivo* in consistent and controlled environments, leading to improved experimental repeatability and high cell viability or molecule activity [14]. Therapeutics within these solid scaffolds may then be surgically implanted by injection, without risk of premature polymerization (e.g., catheter clogging), as the material will thin and flow while stress is applied. After injection and the cessation of stress, the material will self-heal into a gel at the target site.

The majority of shear-thinning and self-healing hydrogels used in biomedical applications are based on amphiphilic peptides that display both a hydrophobic and a charged hydrophilic face [15]. Enthalpic penalty from electrostatic repulsion on hydrophilic faces prevents self-assembly that is driven by the net entropic gain of burying hydrophobic faces together. Repulsion may be negated from pH titration or ionic shielding that act as gelation stimuli. The hydrophobic faces on these peptides then pack together and form

* Corresponding author. University of Pennsylvania, Department of Bioengineering, 240 Skirkanich Hall, 210 S. 33rd Street, Philadelphia, PA 19104, USA. Tel.: +1 215 898 8537; fax: +1 215 573 2071.

E-mail address: burdick2@seas.upenn.edu (J.A. Burdick).

β-sheet sandwiches that grow into entangled fibrils, resulting in a sol–gel transition. Strain fractures the hydrogel into smaller networks, resulting in shear-thinning behaviour, and fractured networks re-intertwine over time, resulting in self-healing behaviour [14]. Other well designed shear-thinning and self-healing systems based on self-repulsive but mutually attractive peptides, multi-block amphiphilic peptides, oppositely charged particles, and protein-ligand associations have been engineered; however, no individual system is without some limitation (e.g., poor gelation kinetics, slow recovery) [10,16–24].

To this end, we strived to develop a hydrogel system that (i) gels quickly under physiological conditions, (ii) is shear-thinning, (iii) recovers rapidly after thinning, (iv) is based on strong and highly-specific cross-linking interactions, and (v) has tunable mechanical and erosion properties. The inherently specific interactions between the docking and dimerization domain (DDD) of cAMP-dependent protein kinase A (PKA) with the anchoring domain (AD) of A-kinase anchoring proteins (AKAP) were exploited to develop such hydrogel materials. DDD-AKAP structural biology has been well studied, which provides us with a strong molecular understanding of DDD-AD interactions and a library of association domains to engineer; however, these precise interactions have not been previously used to engineer hydrogels and materials [25–33]. DDD forms a type-X four-helix bundle that binds to the α-helical and amphipathic AD with strong 1–100 nM affinity [25,26]. The non-covalent associations between AD and DDD may be disrupted with physical force, making hydrogels cross-linked by these interactions speculated to exhibit shear-thinning characteristics. Owing to the rapid nature of AD and DDD binding kinetics, such gels were also expected to self-heal quickly after being thinned. Also, the binding of AD to DDD may be initiated by simply mixing together the two components, allowing gelation to proceed under constant physiological conditions.

Specifically, we designed a recombinant DDD (rDDD) polypeptide consisting of end-blocks derived from RIIα [2–45] PKA linked together with a random-coil spacer mid-block containing RGD integrin binding sites [27,28]. The second component was derived from the anchoring domain of A-kinase anchor protein 13 [1247-1264] (AKAP-LBC) conjugated to the ends of a four or eight arm PEG (4aPEG-AD, 8aPEG-AD) [29]. When mixed together, cross-linking was achieved when multivalent AD domains "lock" onto recombinant dimerization and "docking" domains, in this "Dock-and-Lock" (DnL) self-assembling gelation mechanism. Here, we report on the design of this DnL gel system, as well as characterization of the material tunability, shear-thinning and recovery behavior, and cytocompatability.

2. Material and methods

2.1. PEG-AD synthesis

AD peptide with the sequence *H2N-(ESESLIEEAASRIVDAVIEQVKSESECGGG)-COOH* was synthesized on a Gly-OH functionalized 2-chlorotrityl chloride resin (Novabiochem San Diego, CA) using an automated solid phase peptide synthesizer (PS3, Protein Technologies, Inc, Tucson, AZ). The amino acid residues were activated for coupling with HBTU in the presence of 0.4 M methyl morpholine in DMF and deprotection was carried out in 20% piperidine in DMF for approximately 30 min. Standard cycles of 60 min were used for coupling. The peptide was cleaved from the resin in 95:2.5:2.5 Trifluoroacetic acid (TFA): Triisopropylsilane (TIPS): water for 3–4 h, precipitated with the addition of excess ether, and pelleted by centrifugation at 4,000 g for 10 min. Ether was decanted and removed by vacuum, and the peptide was used directly or frozen and lyophilized for storage. The identity of the peptide was confirmed with MALDI-TOF mass spectroscopy (ABI PerSeptive Voyager, Framingham, MA; Philadelphia Wistar Proteomics Facility). The AD peptide was conjugated to 10 kDa four arm PEG (4aPEG)-maleimide or 20 kDa eight arm PEG (8aPEG)-maleimide (Jenkem Technology USA) via Michael-type addition reaction between peptide cysteine and PEG maleimide in degassed buffer at pH 7.0 overnight, using a 3-fold molar excess of peptide to maleimide groups. The product was isolated by dialysis (6 kDa MWCO dialysis tubing) and lyophilization, and the extent of the reaction between PEG-maleimide and AD peptide was determined by ^{1}H NMR (Bruker), through comparison and calibration of hydrogen shifts on L, V, and I at ∼1 ppm with the hydrogen shifts on PEG at ∼3.75 ppm. A similar approach was used to synthesize an alternate peptide, termed AD-0, with a sequence of *ESESQIEYLAKQIVDNAIQQASESECGG*.

2.2. Cloning and expression of rDDD

The DNA sequence for rDDD, optimized for expression in *E. Coli*, was synthesized and cloned in pJExpress411 expression plasmid by DNA2.0 Inc. (CA, USA). rDDD was expressed in lactose induced cultures with the Studier autoinduction method (Fig. S1) [34]. For expression of the polypeptide, the recombinant plasmid, rDDD-pJExpress411, was transformed into *rne131 E. coli* expression strain BL21Star™(DE3) (Invitrogen). A single colony BL21Star™(DE3) containing rDDD-pJExpress411 was inoculated in 5 ml sterile LB media containing 30 μg/ml kanamycin and grown overnight. 1 ml of the overnight culture was subsequently used to inoculate 500 ml of ZYP-5052 media for autoinduction of protein expression. The 500 ml cultures were grown in a shaker at 37 °C for 4–5 h until the OD$_{600}$ reached 0.8 and then grown at 25 °C with constant shaking for an additional 24 h. Protein expression was monitored by sodium dodecyl sulfate polyacrylamide gel electrophoresis (SDS-PAGE) of samples with normalized OD$_{600}$ and visualized via Coomassie blue staining. Cells were harvested by centrifugation (10,000 g for 15 min at 4 °C), stored at −80 °C until use, and then thawed and lysed by resuspension in 100 mM NaH$_2$PO$_4$, 10 mM Tris·Cl, 8 M urea, 1% triton X-100, pH 8.0 (buffer A) and disruption on ice using an Ultra Sonic Dismembrator (10 mm tapered horn) for 15 min with cycles of 30 s bursts and 30 s cooling time. The cell lysate was centrifuged at 16,000 g for 60 min and the supernatant was carefully decanted. Clarified lysate was passed through a Ni-Sepharose HisTrap FF column (GE Healthcare) equilibrated with buffer A. Unbound protein was washed with three column volumes of buffer A. Denaturant was removed by three column volume washes of 50 mM sodium phosphate, 300 mM NaCl, 20 mM imidazole, pH 8.0 native buffer. Protein was eluted by five column washes of native buffer containing 500 mM imidazole. Purified protein was concentrated and buffer exchanged to deionized water via ultrafiltration across a 10 kDa NMWL regenerated cellulose membrane (Amicon Ultracel, Millipore). Protein was frozen and lyophilized to yield a white fluffy solid. The molecular weight of the purified protein was confirmed via SDS-PAGE and MALDI-TOF mass spectrometry.

2.3. Gel formation

Stock PEG-AD and rDDD were separately dissolved in PBS or hMSC growth medium (αMEM supplemented with 16.67% FBS, 1% L-glutamine, and 1% Penicillin/Streptomycin). To initiate gelation with the DnL self-assembly mechanism, the two components were simply mixed together (Fig. 1). To provide insight into the DnL gel molecular architecture, gels were flash frozen in liquid nitrogen and imaged with scanning electron microscopy (FEI Quanta 600 Environmental FE-SEM, Oregon).

2.4. Rheology

Dynamic oscillatory time, frequency and strain sweeps were performed using an AR2000 stress-controlled rheometer (TA Instruments, New Castle, DE) with 20 mm diameter cone and plate geometry, 59 min 42 s cone angle, and at a 27 μm gap distance. To form the gels, stock suspensions of PEG-AD and rDDD were made in PBS at the desired pH. These solutions were then mixed together to form gels with specified compositions and the gel was applied between the 2 plates of the rheometer. The top plate was lowered to a 27 μm gap distance and excess gel was scraped off. Care was taken to achieve a homogeneous distribution of gel within the top and bottom plates of the rheometer. Dynamic oscillatory time sweeps were collected at angular frequencies of 6.3 rad s^{-1} and 0.5% strain. An initial strain amplitude sweep was performed at 25 °C at different frequencies to determine the linear viscoelastic range for the gel. Rheological properties were examined by frequency sweep experiments ($\omega = 0.1$–100 rad s^{-1}) at a fixed strain amplitude of 0.5%. Experiments were repeated on 3 to 4 samples and representative data is presented. For shear recovery experiments at 6.3 rad s^{-1}, shear thinning was induced via application of 500% strain for 2 min. The strain was released to 0.5% for 3 min to allow the gel to recover.

2.5. Circular dichroism spectroscopy

Circular dichroism (CD) spectra were obtained with a Jasco (Easton, MD) J-810 Spectropolarimeter connected with a Peltier temperature controller. Samples were analyzed in a 1 mm quartz cuvette in pH 7.4 or 4.2 PBS at 25 °C and 50 nm min^{-1}, with 1 nm pitch, 1 nm bandwidth, and 4 s response time. AD and rDDD were measured at 0.5 mg mL^{-1}, and mixed samples contained 0.125 mg mL^{-1} AD with 0.5 mL^{-1} rDDD (yielding approximately 3 AD domains per 2 rDDD domains). A mean residue weight of 106.86 was used to convert measurements into mean residue elipticities for mixed AD + rDDD samples. Reported spectra are the average of three scans.
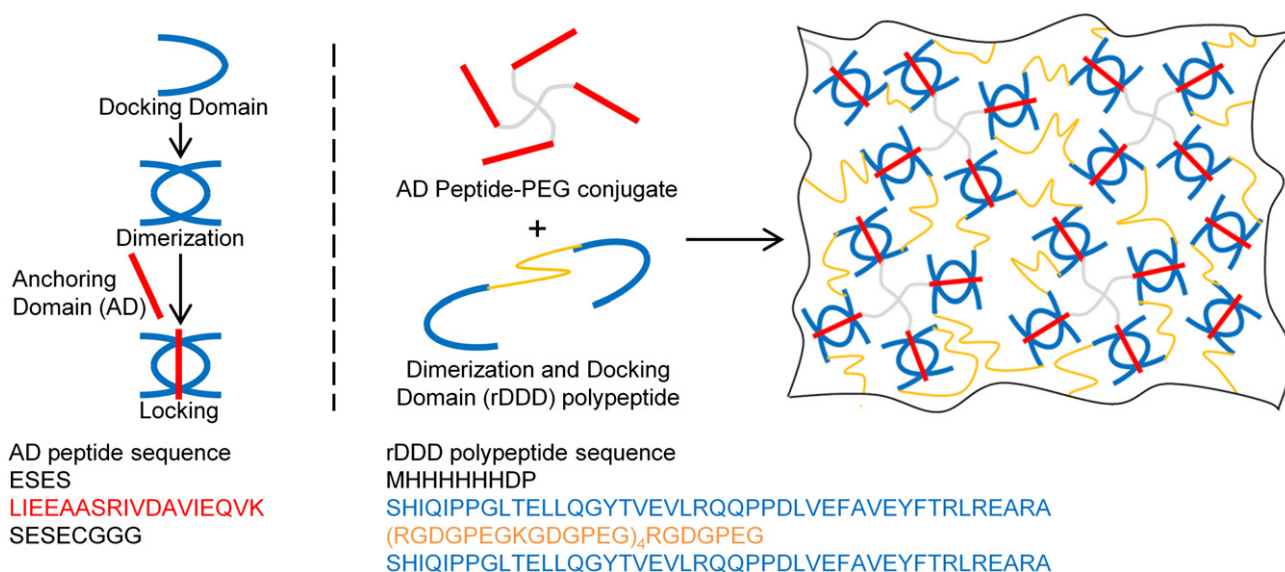
Fig. 1. Dock-and-Lock self-assembly mechanism. Docking domains dimerize and lock with the anchoring domain (left). Engineered anchoring domains and docking domains self-assemble to form dynamic, shear-thinning, self-healing hydrogels when mixed (right).

2.6. Hydrogel erosion

Acrylamide molds were fabricated with a 12 mm high and 15 mm diameter wide cavity and containing a 6 mm high and 5 mm wide depression in the center. Molds were washed with PBS and dried, and stock solutions of the crosslinker and rDDD were mixed into the depression to form 40 µL gels of the desired composition. Solutions of 8aPEG-AD containing 0.1 wt% fluorescein isothiocyanate conjugated dextran (FITC-dex, MW 500,000; Sigma) were used for mock drug encapsulation and release studies. Gels were gently centrifuged at 500 g for 1 min to level gel surfaces. Gels were covered in 1 mL PBS and allowed to erode for specified time periods, whereupon solutions above the intact gels were gently aspirated and stored at $-20\,^{\circ}$C. Solutions were then replaced with 1 mL fresh PBS, and this process was repeated until gels were completely eroded. Care was taken to ensure sterility throughout. Protein concentrations in collected solutions were determined by absorbance at 280 nm, and the FITC-dex concentration was determined by emission fluorescence at 520 nm after excitation at 490 nm. FITC absorbance at 495 nm was taken and used to correct protein absorbance ($A_{280}^{FITC} = A_{495}^{FITC}/3$) for samples containing both dextran and eroded gel. Reported profiles are based on erosion averages of three gels for each specified composition.

2.7. Hydrogel cytocompatibility

hMSCs (Lonza) were expanded to passage 4 in standard hMSC growth medium. hMSCs were resuspended in hMSC growth media and mixed with PEG-AD dissolved in the same media. The hMSC/PEG-AD solution was pipetted into a barrel of a syringe, and rDDD in hMSC growth media was then pipetted into the same barrel and gently mixed to induce gel formation. All encapsulation studies were performed with 5×10^6 cells mL^{-1} in 3 wt% 8aPEG-AD - 4.5 wt% rDDD gels. Gels were extruded through a 21-gauge needle directly into a 96-well plate or into a pre-formed collagen gel (PurCol; Advanced Biomatrix), covered with excess hMSC media, and imaged either 24 h or 3 days later. To assess viability, constructs were rinsed with PBS, stained with a live/dead kit consisting of calcein AM and ethidium homodimer (Invitrogen), and visualized using confocal microscopy. Constructs were excited at 488 nm and 543 nm wavelengths to visualize live and dead cells, respectively, and z-stacks were taken through the depth of the gels to validate an even distribution of cells throughout. Experiments were performed in triplicate and viability is reported as the percentage of calcein stained cells compared to total cells.

3. Results

3.1. DnL component production

AD peptide was successfully synthesized (representative MALDI-TOF spectra shown in Fig. S2) and conjugated to multi-arm PEG. Molar conjugation efficiencies were similar for both four arm (4aPEG-AD, 0.76 peptides per 1 PEG arm) and eight arm PEG (8aPEG-AD, 0.81 peptides per 1 PEG arm), as determined by ^{1}H

NMR (Fig. S3). rDDD was successfully expressed with a T7 promoter system and was isolated to over 95% purity with yields as high as 75 mg L^{-1} culture (representative MALDI-TOF spectra and SDS-PAGE shown in Fig. S4).

3.2. DnL hydrogel gelation

Neither 4aPEG-AD nor 8aPEG-AD formed gels alone in pH 7.4 PBS at 6 wt% (Fig. 2). However, these components formed hydrogels with neutralization of the AD peptide surface charge, indicated by the increase of material storage modulus (G′) over material loss modulus (G″) at decreased pH (Fig. S5–S7). rDDD did not form gels alone at 6 wt% or in the presence of 4 wt% unmodified 4aPEG (Fig. 2, S8). However, upon mixing rDDD with PEG-AD to a final 3 wt% 4/8aPEG-AD and 4.5 wt% rDDD composition (resulting in approximately 2 AD domains per one rDDD domain) gelation was observed
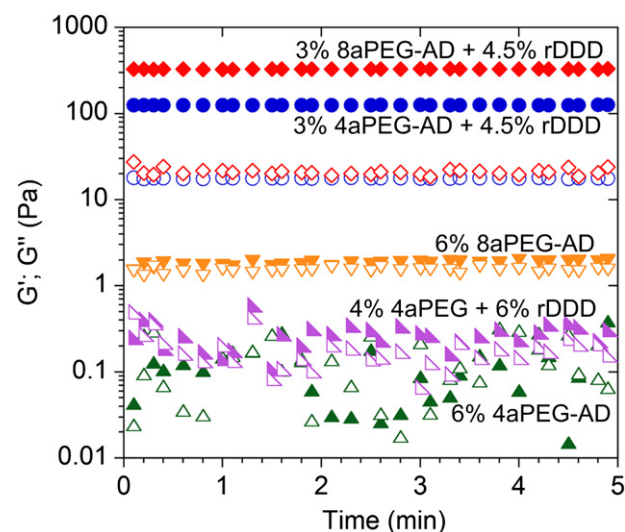
Fig. 2. Oscillatory time sweeps of DnL materials. Storage modulus (filled symbols) and loss modulus (empty symbols) of PEG-AD components alone, rDDD with unmodified 4aPEG, and rDDD with PEG-AD (4aPEG-AD and 8aPEG-AD). Sweeps were performed at 0.5% strain and 6.3 rad s^{-1}.

immediately (<1 s). The pH of the DnL components and assembled gel was ensured to be at 7.4 from pH paper tests, to make sure gelation was not an artifact of an unintended pH shift. rDDD also formed hydrogels when mixed with multi-arm PEG conjugated to other anchoring domains (AD-0) (Fig. S8), but studies with AD-0 are not emphasized here because AD-0 exhibited limited solubility and tended to form weak gels by itself at high concentrations. Flash frozen and lyophilized DnL gels exhibited a networked and porous structure (Fig. S9).

AD at pH 7.4 exhibited a combination of random-coil and α-helical secondary structures, shown by the double minima near 208 nm and 222 nm (indicative of α-helical conformation) and net negative elipticity below 200 nm (indicative of random-coil conformation) in the CD spectra (Fig. S10). At pH 4.2, AD was more helical, shown by the decreased negative elipticity between 200 nm and 260 nm. rDDD also showed both random-coil and α-helical conformations. When mixed with AD (to approximately 1.4 AD per 1 rDDD), the resultant CD spectra was not the simple addition of AD and rDDD spectra (especially evident at wavelengths below 200 nm) and indicated an overall increase in helical content.

3.3. DnL gel mechanics and erosion

Mixing PEG-AD and rDDD together resulted in the immediate formation of soft and elastic hydrogels, for both 4aPEG-AD and 8aPEG-AD (Fig. 2). Gel moduli were highly dependent on oscillatory deformation frequency, and were more elastic at high shear rates, but were more viscous at low shear rates (Fig. 3). DnL gels with variable rheological properties could be constructed by mixing DnL components to different final compositions. Increasing the concentration of DnL components, while keeping the ratio of DnL to PEG-AD (for both 4aPEG-AD and 8aPEG-AD) constant, led to an increase in G′ and G″ with minimal effect on gel relaxation time and modulus frequency dependence (Fig. 3A and B). Gels with plateau G′ as low as ~10 Pa (5 wt%) and as high as ~1000 Pa (10 wt%) were formed. In reference to regimes where the AD to rDDD molar ratio is not close to one (2 wt% PEG-AD and 3 wt% rDDD; ~2 AD per rDDD), increasing the molar ratio of rDDD to PEG-AD while keeping PEG-AD wt% constant (2 wt% PEG-AD and 4.5 wt% rDDD; ~1.33 AD per rDDD), increases plateau G′ and G″, lowers the relaxation time of hydrogels, and rendered them vulnerable to deformation at lower shear rates (Fig. 3C and D). In reference to regimes where the AD to rDDD molar ratio is near one (2 wt% PEG-AD and 4.5 wt% rDDD), further varying the gel composition to have one to one AD to rDDD ratio (2 wt% PEG-AD and 6 wt% rDDD) had relatively little effect on moduli, relaxation times, and shear-thinning properties. Relaxation times of DnL gels were highly variable, and ranged from around 0.1–1 s⁻¹.

Increasing the PEG-AD arm valency from four to eight led to an increase in both hydrogel moduli and relaxation times (Fig. 3A and B). However, DnL gels made with 8aPEG-AD had yield strains (~100%) that were approximately half that of gels made with 4aPEG-AD (~200%) (2 wt% PEG-AD and 3 wt% rDDD gels) (Fig. 4A
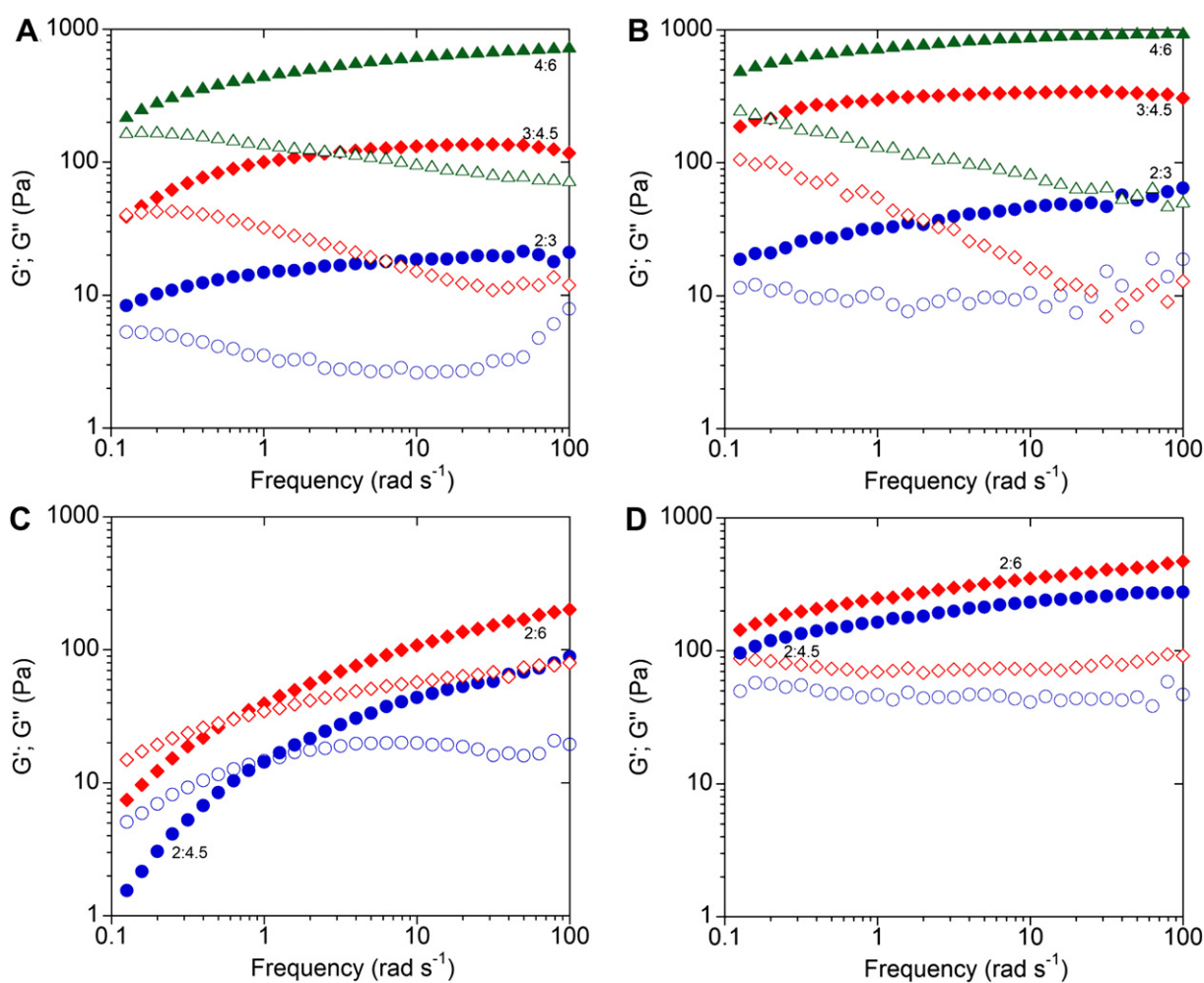
Fig. 3. Oscillatory frequency sweeps of DnL hydrogels. (A, C) storage modulus (filled symbols) and loss modulus (empty symbols) of DnL gels at various 4a-PEG-AD:rDDD. (B, D) modulus of analogous of DnL gels constructed with 8a-PEG-AD. Sweeps were performed at 0.5% strain.

and B). Increasing the PEG-AD to rDDD molar ratio resulted in a proportionally increased yield strain for both 8aPEG-AD (~200%) and 4aPEG-AD (~400%) (2 wt% PEG-AD and 6 wt% rDDD gels) (Fig. 4). Regardless, all DnL gels still displayed extraordinary resistance to strain-induced deformation. When subjected to 500% strain over time, all DnL gels underwent gel–sol transition and behaved as liquids, as expected from recorded strain sweep curves. However, upon lowering oscillatory strain from 500% to 0.5%, thinned DnL gels rapidly underwent sol–gel transition and recovered back to their initial moduli immediately (<6 s, the minimum time between each data point on the rheometer) (Fig. 5, S11). All DnL gels were capable of self-healing to their original state without showing any signs that mechanical fidelity was compromised, irrespective of the number of times they were previously shear-thinned. Hydrogels formed with AD-0 were similarly shear-thinning and self-healing, but exhibited higher moduli and pseudoplasticity (Fig. S12-S14). A summary of gel rigidity for all formulations investigated is provided in supplementary information (Table S1).

DnL gels eroded initially at relatively high rates, followed by slower and nearly linear rates (Fig. 6). Erosion rates of DnL gels were also tunable. Increasing the locking domain molecular valency decreased erosion rates; 3 wt% 4aPEG-AD − 4.5 wt% rDDD gels required ~5 days to erode 90%, while 3 wt% 8aPEG-AD − 4.5 wt% rDDD gels required ~15 days to erode 90% (Fig. 6A). By adjusting

the molar ratio of AD to rDDD domains closer to one, erosion rates also decreased (e.g., 2 wt% 8aPEG-AD − 4.5 wt% rDDD gels required ~35 days to completely erode). However, the erosion rates of DnL gels were minimally affected by changing the total gel weight if AD to rDDD molar ratios remained constant (5 wt% total compared with 7.5 wt% total). The erosion rates were also only minimally affected when gels were supplemented with dextran and the release of encapsulated dextran correlated with the erosion rates of DnL gels (Fig. 6B).

3.4. Cell encapsulation and delivery with DnL gels

PEG-AD and rDDD dissolved in hMSC growth medium (containing serum) behaved the same as when dissolved in PBS, and still formed hydrogels when mixed together. This was taken advantage of to rapidly encapsulate cells under constant physiological conditions, by dissolving DnL components in hMSC containing media and mixing them together. Cells encapsulated in this manner were then delivered by thinning the gel through a 21-gauge needle from injection. Importantly, cells were highly viable (93.0 ± 3.1%), and remained homogenously encapsulated after injection and gel-recovery (Fig. 7A). When delivered into a collagen gel (acting as a mock collagenous tissue), hMSCs remained similarly highly viable (91 ± 4.8%) and homogenously encapsulated even
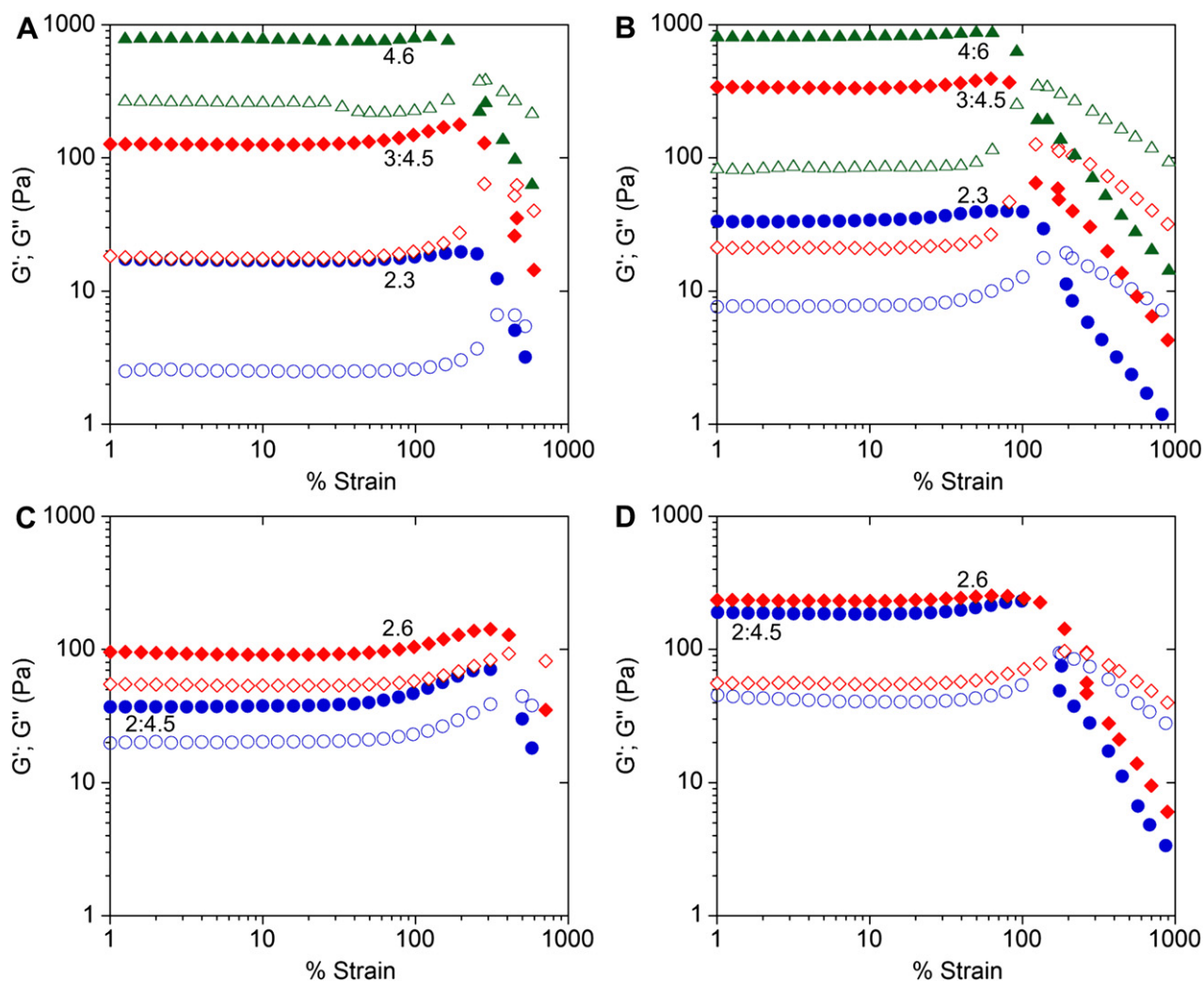
Fig. 4. Oscillatory strain sweeps of DnL hydrogels. (A, C) storage modulus (filled symbols) and loss modulus (empty symbols) of DnL gels at various 4a-PEG-AD:rDDD wt%, (B, D) and that of gels at various 8a-PEG-AD:rDDD wt%. Sweeps were performed at 6.3 rad s^{-1}.
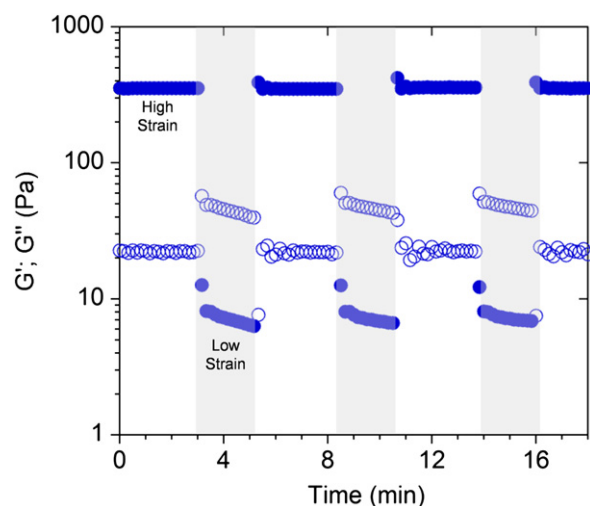
Fig. 5. DnL hydrogel deformation and recovery. Storage modulus (filled symbols) and loss modulus (empty symbols) of 3 wt% 8aPEG-AD − 4.5 wt% rDDD gels evolving over time from repeated cycles of 3 min low 0.5% strain and 2 min high 500% strain oscillations at 6.3 rad s^{-1}.

after culture for three days (Fig. 7B). Note that detector gain and amplifier offset needed to be increased when visualizing cells in collagen gels to accommodate for the presence of collagen, which led to the visual artifact of vertically stretched cells in constructed Z-stacks.

4. Discussion

We have constructed a DnL hydrogel system using molecular engineering to meet strict criteria for a self-assembling and shear-thinning material that has potential utility for applications in drug and cell delivery. This two-component system was designed through the interactions of the RIIα subunit of cAMP-dependent kinase A and the anchoring domain of A-kinase anchoring protein (AKAP). Our original design consisted of AKAP-IS, an anchoring domain engineered with bioinformatics methods to bind rDDD with an exceptional 0.45 nM affinity [26]; however, AKAP-IS exhibited poor solubility in solution. The peptide was then modified with flanking ESES amino acids to improve solubility (termed AD-0); however, when conjugated to multi-arm PEG, this peptide tended to form weak gels at high concentrations at pH 7.4. Further studies of gels formed with AD-0 were performed, (Fig. S8, S12−S14) but we sought to engineer DnL components that did not gel in isolation at physiological conditions, but rather only when the two components were mixed.

Analysis of the AKAP-IS crystal structure revealed that AKAP-IS exhibits an α-helical structure with a neutral hydrophilic face and a hydrophobic face (Fig. S15) [25]. This amino acid arrangement may lead to the stacking of hydrophobic−hydrophobic and hydrophilic−hydrophilic faces, which likely resulted in weak peptide association, cross-linking, and weak gelation of PEG-AD-0. Substitution of hydrophobic amino acids into hydrophilic ones to improve solubility was not possible, as such changes eliminated binding affinity to DDD [25]. Structural analysis of other anchoring domains led us to AKAP-LBC, which has an α-helical structure with a negatively charged hydrophilic face that still bound to DDD with 2.2 nM affinity (Fig. S15) [26]. We postulated that the net charge on the peptide's face would limit peptide stacking, and the addition of the same charged hydrophilic flanking amino acids would further assist in preventing peptide aggregation and undesired gelation after conjugation to multi-arm PEG. ESES was chosen as a flanking

modifier because it is also negatively charged, displays steric flexibility, and could be titrated to remove electrostatic repulsion if desired, resulting in the design of AD. This AD construct did not form gels in PBS at physiological pH (Fig. 2). If the full solubility of PEG-AD was endowed due to our design of utilizing surface charge to limit undesired peptide interactions, then these peptide interactions could be reinstated when surface charge was removed. This allows PEG-AD to be cross-linked by triggering AD−AD associations by charge removal from pH titration. Indeed, we observed gelation of PEG-AD with decreasing pH, and sol to gel and gel to sol transitions were repeatedly cycled by cycling between acidic and neutral pH (Fig. S5-S6). CD spectra indicated that AD has a mixture of α-helical and random-coil structure, as is expected from the combination of the native helical structure of AD and its unstructured flanking modifications (Fig. S10). When titrated to lower pH, the peptide shows increased helicity, consistent with the postulation that helical bundles formed at lower pH. β-sheet forming self-assembling peptides whose gelation can be similarly triggered by charge removal via pH titration have already been engineered; however, we have developed a pH sensitive gelation mechanism based on modifying a naturally found α-helical motif, and this modified peptide has a dual functionality of both triggerable self-
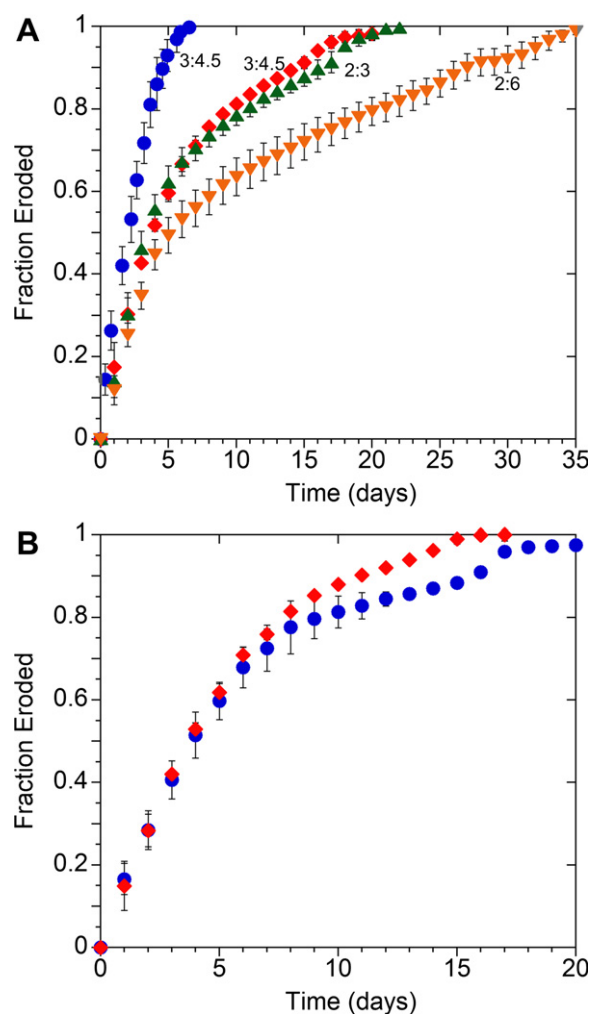
Fig. 6. DnL hydrogel erosion. (A) fraction of gels eroded over time, with DnL gels constructed with various PEG-AD:rDDD wt%, using both 4aPEG-AD (blue circles) and 8aPEG-AD (all other groups). (B) fraction of 3 wt% 8aPEG-AD − 6.0 wt% rDDD hydrogel containing dextran eroded (blue circles) and fraction of encapsulated dextran released (red diamonds) over time. (For interpretation of the references to colour in this figure legend, the reader is referred to the web version of this article.)
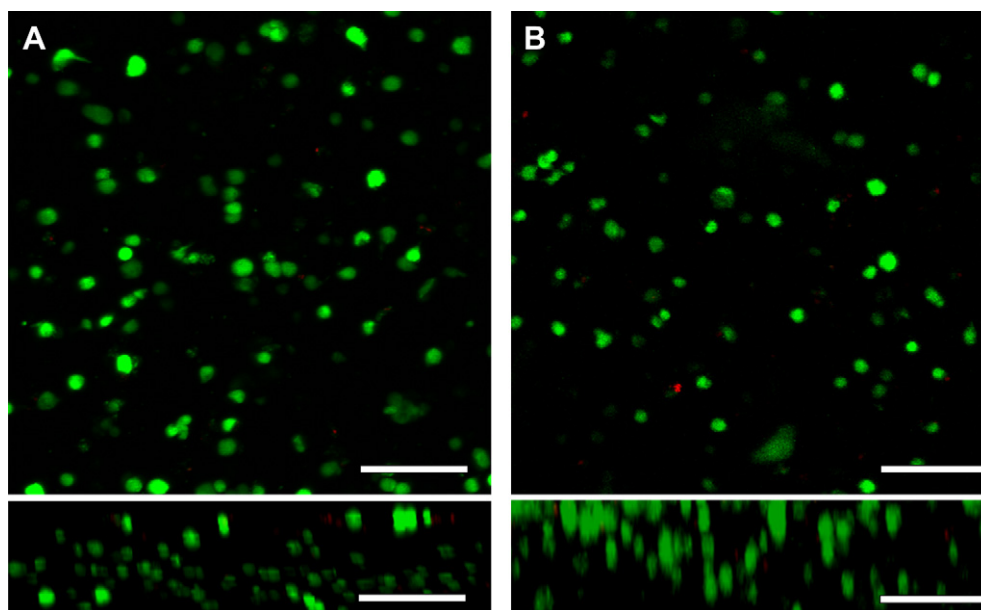
Fig. 7. Cell delivery in DnL hydrogels. (A) top-down and side views of confocal microscopy images, showing viability (viable cells: green, dead cells: red) and spatial distribution of hMSCs encapsulated in DnL gels and injected into a 96 well plate after 24 h culture. (B) top-down and side views of confocal microscopy images of hMSCs encapsulated in DnL gels and injected into a collagen gel after 3 days culture. (For interpretation of the references to colour in this figure legend, the reader is referred to the web version of this article.)

assembly and specific affinity towards a target protein. This strategy of end-functionalizing charged and flexible motifs on initially poorly soluble α-helical domains can be broadly applied to engineer constructs that can self-assemble on demand.

Gelation triggered by the facile mixing of disparate components is an attractive method to encapsulate therapeutic cargo at constant physiological conditions. We designed a recombinant and dimeric docking domain (rDDD) that was used to cross-link PEG-AD when mixed together for the engineering of such a gelation mechanism. The two docking domains are linked together by a flexible hydrophilic spacer, to limit steric constraints that would prevent AD binding. While rDDD and PEG-AD were slightly viscous solutions in PBS or hMSC culture media in isolation at 6 wt% in the timescale of experiments, they immediately formed hydrogels when mixed together without the use of any other exogenous milieu (Fig. 2). CD spectra of rDDD revealed that rDDD had both α-helical and random-coiled domains, as is anticipated from the natural helical structure of DDD and unstructured polypeptide linker (Fig. S10). rDDD mixed with AD had an overall higher helical content than rDDD or AD in isolation, implicating that tetrameric coiled helical bundles were formed and supporting the notion that the DnL gelation mechanism is based on rDDD/AD binding interactions. The binding is inherently highly specific, and gelation was not deterred nor initiated by serum, other components found in growth medium, or unmodified PEG. Gelation kinetics could not be accurately investigated because the moduli evolution to steady state was too rapid to be captured on a rheometer. In contrast, many other peptide-based shear-thinning systems require upwards of a few hours for gelation and evolution to steady state moduli, likely due to the stepwise peptide self-assembly and incremental fibril growth necessary for entanglement and gelation, whereas a single protein-binding event is the only step required for DnL cross-linking [19,24,35].

Gels with G′ up to ∼ 1000 Pa were produced (≤10 wt%), which is significantly more rigid than other gels constructed with comparable systems based on protein-ligand interactions (from 1 to 50 Pa), owing likely to the naturally strong affinity of DnL interactions [18,36]. DnL gels behaved similarly to other materials with conventional transient networks, and exhibited elastic gel-like properties at high frequencies, and viscous liquid-like behavior at lower frequencies (Fig. 3). The gels were shear-thinning and pseudoplastic, and could be thinned into liquid form with extended or excessive shear-strain. DnL gels were highly resilient to strain-induced deformation, and were able to sustain strains as high as 400% prior to yielding, which is over 1-2 orders of magnitude higher than that of other shear-thinning gels (Fig. 4) [16,21,35]. Upon deformation and removal of deformation stress, DnL gels were capable of quickly recovering back into gel form. The rheological recovery profile could not be accurately detailed because it also occurred too rapidly; however, complete gel recovery to its original modulus was observed in as little as 6 s (Fig. 5). This recovery time is also much faster than other comparable shear-thinning systems, which require minutes to hours [18,19,24,35,37]. To support the rapid nature of DnL self-recovery, the relaxation times of DnL gels ranged from only ∼0.1−1 s, and are 2−4 orders of magnitude lower than comparable telechelic polypeptide hydrogels based on leucine-zipper domains and collagen-like domains [38,39]. As with the rapid gelation kinetics, the fast recovery rates of DnL gels likely stems from the inherently rapid on rates of AD/rDDD binding and single-step binding for cross-link formation, instead of requiring multistep and passive fibril growth and re-entanglement for self-healing. DnL gels recovered back to their original modulus regardless of the number of times or extent of deformation. DnL gels with compositions studied here required weeks upward to a month to completely erode under the conditions investigated. Erosion and degradation rates of hydrogels are important cell and drug delivery parameters, and the erosion rate of DnL gels are slow compared to many other hydrogels based on uni-specific and non-covalent interactions, many of whom completely erode within hours [39−43].

The ability to control gel mechanics and physical properties are integral for directing encapsulated cargo behavior and therapeutic benefit [44]. DnL gels exhibited a remarkable range of physical properties from molecular design of DnL components. By appropriately varying DnL component concentrations, ratios, and PEG-AD valency, gel rigidity, relaxation times, yield strain, modulus-

stress frequency relationships, and modulus-strain relationships were independently changed. By keeping DnL component ratios constant but increasing the total gel wt%, gel network density increased while retaining similar molecular architecture; as a consequence, DnL gels exhibit variable rigidity while retaining similar relative moduli-frequency/moduli-strain dependencies and erosion rates, from tuning gel wt% (Figs. 3A-B, 4A-B, 5). When compared to 4aPEG-AD, 8aPEG-AD led to increased networking from increased molecular branching, observed by the formation of less dynamic gels with higher G', greater resistance to deformation over long shear rates, and decreased erosion rates (Figs. 3A–C, 5). However, as a consequence of decreasing the relative number of discrete PEG-AD molecules by half with 8aPEG-AD (compared with 4aPEG-AD at equal PEG-AD wt%), the flexibility of PEG-AD to rearrange itself to accommodate high strains is reduced, and this is reflected by the decreased yield strain of 8aPEG-AD DnL gels (Fig. 4A–C). Modulating PEG-AD valency thus offers an avenue to tune gel rigidity, pseudoplasticity, brittleness and erosion rate. Increasing the relative number of rDDD to PEG-AD from varying component ratios results in greater molecular rearrangement flexibility, as represented by an increase in yield strains with gels formed with higher rDDD to PEG-AD molar ratios (at constant PEG-AD content) (Fig. 4). Additionally, the rate kinetics of PEG-AD binding with rDDD should be higher due to increased rDDD concentration (at constant PEG-AD concentration), as represented by the decreased relaxation time of such hydrogels with higher rDDD content (Fig. 3). When there is a molar excess of one DnL component, the addition of the second component also leads to additional cross-linking and network formation, resulting in increased plateau moduli and decreased erosion rates. Thus, DnL component ratios can be manipulated to tune gel rigidity, brittleness, relaxation time, and erosion rate. Additionally, anchoring domains with higher affinity and more rapid association rates with rDDD could be used to form gels with higher rigidity (reflective of increasing binding strength) and decreased relaxation times (reflective of fast on rate kinetics) (Fig. S12–S14).

The biomedical value of DnL gels were assessed from studying the potential of DnL gels to act as drug and cell delivery vehicles. Cells and drugs were very rapidly and homogenously encapsulated *ex vivo* at constant physiological conditions (in either PBS or cell media) by simply suspending them with one DnL component and mixing in the second DnL component, affirming the systems controllable, specific, and yet mild encapsulation mechanism. DnL gel's shear-thinning and self-healing properties make such *ex vivo* formed gels injectable to *in situ* sites, from thinning through a fine needle. Importantly, sensitive cargo such as hMSCs survived this delivery process, and gel-recovery rates were rapid enough to ensure cells stayed homogenously encapsulated after injection and delivery. This attests that DnL gels are injectable, cytocompatible, self-supporting cell carriers (Fig. 7). Additionally, the release profile of large encapsulated cargo corresponded with the erosion rate of DnL gels (Fig. 6B). Thus, the erosion rate of DnL gels can also be manipulated to control drug and cell release rates in therapeutic applications. Although preliminary and evaluation and optimization will need to be performed with a specific application in mind, these studies illustrate the wide potential of DnL gels in regenerative medicine, and future *in vivo* cell and drug delivery studies will provide additional insight in the roles that DnL gels may play in medical applications.

5. Conclusions

In summary, we have a engineered a dual-component Dock-and-Lock self-assembling gelation mechanism that can be utilized to form injectable hydrogels that can be triggered to quickly gel at constant physiological conditions, are shear-thinning, rapidly recovering, cytocompatible, based on highly-specific interactions, and whose physical properties are highly tunable. These characteristics allow therapeutic cargo to be encapsulated in DnL gels and delivered with minimally invasive techniques, while minimizing issues concerning deleterious gelation stimuli, cargo diffusion away from injection target sites, inhomogeneous cargo encapsulation, delivery failure from catheter clogging, and experimental repeatability. DnL gels have exceptional properties, such as immediate gelation rates, immediate self-recovery rates, remarkable tolerance to high strains, and outstanding potential to self-heal from mechanical abuse. DnL gel properties can be highly tuned, and we outline the molecular basis of observed macroscopic rheological behavior.

Appendix. Supplementary information

Supplementary information associated with this article can be found, in the online version, at doi:10.1016/j.biomaterials.2011.11.076.

References

[1] Ratner BD, Bryant SJ. Biomaterials: where we have been and where we are going. Ann Rev Biomed Eng 2004;6:41–75.
[2] Yu L, Ding J. Injectable hydrogels as unique biomedical materials. Chem Soc Rev 2008;37:1473–81.
[3] Nguyen MK, Lee DS. Injectable biodegradable hydrogels. Macromol Biosci 2010;10:563–79.
[4] Tan H, Marra KG. Injectable, biodegradable hydrogels for tissue engineering applications. Materials 2010;3:1746–67.
[5] Jeong B, Bae YH, Lee DS, Kim SW. Biodegradable block copolymers as injectable drug-delivery systems. Nature 1997;388:860–2.
[6] Mano JF. Stimuli-responsive polymeric systems for biomedical applications. Adv Eng Mater 2008;10:515–27.
[7] Petka WA, Hardin JL, McGrath KP, Wirtz D, Tirrell DA. Reversible hydrogels from self-assembling artificial proteins. Science 1998;281:389–92.
[8] Chung HJ, Park TG. Self-assembled and nanostructured hydrogels for drug delivery and tissue engineering. Nano Today 2009;4:429–37.
[9] Nair LS, Laurencin CT, Tandon M. Injectable hydrogels as biomaterials. In: Basu B, Katti DS, Kumar A, editors. Adv biomaterials: Fund Proces App; 2009. p. 179–203.
[10] Gupta D, Tator CH, Shoichet MS. Fast-gelling injectable blend of hyaluronan and methylcellulose for intrathecal, localized delivery to the injured spinal cord. Biomaterials 2006;27:2370–9.
[11] Martens TP, G AFG, Parks JJ, Vunjak-Novakovic G. Percutaneous cell delivery into the heart using hydrogels polymerizing in situ. Cell Transplant 2009;18:297–304.
[12] Yan CQ, Pochan DJ. Rheological properties of peptide-based hydrogels for biomedical and other applications. Chem Soc Rev 2010;39:3528–40.
[13] Guvendiren M, Lu HD, Burdick JA. Shear-thinning hydrogels for biomedical applications. Soft Matter 2012;8:260–72.
[14] Yan CQ, Altunbas A, Yucel T, Nagarkar RP, Schneider JP, Pochan DJ. Injectable solid hydrogel: mechanism of shear-thinning and immediate recovery of injectable beta-hairpin peptide hydrogels. Soft Matter 2010;6:5143–56.
[15] Hamley IW. Self-assembly of amphiphilic peptides. Soft Matter 2011;7:4122–38.
[16] Bakota EL, Wang Y, Danesh FR, Hartgerink JD. Injectable multidomain peptide nanofiber hydrogel as a delivery agent for stem cell secretome. Biomacromolecules 2011;12:1651–7.
[17] Wang Q, Wang L, Detamore MS, Berkland C. Biodegradable colloidal gels as moldable tissue engineering scaffolds. Adv Mater 2008;20:236–9.
[18] Foo CTSWP, Lee JS, Mulyasasmita W, Parisi-Amon A, Heilshorn SC. Two-component protein-engineered physical hydrogels for cell encapsulation. Proc Natl Acad Sci USA 2009;106:22067–72.

[19] Haines-Butterick L, Rajagopal K, Branco M, Salick D, Rughani R, Pilarz M, et al. Controlling hydrogelation kinetics by peptide design for three-dimensional encapsulation and injectable delivery of cells. Proc Natl Acad Sci USA 2007; 104:7791–6.

[20] Kiick KL. Peptide- and protein-mediated assembly of heparinized hydrogels. Soft Matter 2007;4:29–37.

[21] Ramachandran S, Tseng Y, Yu YB. Repeated rapid shear-responsiveness of peptide hydrogels with tunable shear modulus. Biomacromolecules 2005;6: 1316–21.

[22] Pochan DJ, Schneider JP, Kretsinger J, Ozbas B, Rajagopal K, Haines L. Thermally reversible hydrogels via intramolecular folding and consequent self-assembly of a de novo designed peptide. J Am Chem Soc 2003;125: 11802–3.

[23] Rajagopal K, Lamm MS, Haines-Butterick LA, Pochan DJ, Schneider JP. Tuning the pH responsiveness of beta-hairpin peptide folding, self-assembly, and hydrogel material formation. Biomacromolecules 2009;10:2619–25.

[24] Ozbas B, Kretsinger J, Rajagopal K, Schneider JP, Pochan DJ. Salt-triggered peptide folding and consequent self-assembly into hydrogels with tunable modulus. Macromolecules 2004;37:7331–7.

[25] Gold MG, Lygren B, Dokurno P, Hoshi N, McConnachie G, Taskén K, et al. Molecular basis of AKAP specificity for PKA regulatory subunits. Mol Cell 2006;24:383–95.

[26] Alto NM, Soderling SH, Hoshi N, Langeberg LK, Fayos R, Jennings PA, et al. Bioinformatic design of A-kinase anchoring protein-in silico: a potent and selective peptide antagonist of type II protein kinase A anchoring. Proc Natl Acad Sci USA 2003;100:4445–50.

[27] Newlon MG, Roy M, Morikis D, Hausken ZE, Coghlan V, Scott JD, et al. The molecular basis for protein kinase A anchoring revealed by solution NMR. Nat Struct Biol 1999;6:222–7.

[28] Foss KB, Solberg R, Simard J, Myklebust F, Hansson V, Jahnsen T, et al. Molecular cloning, upstream sequence and promoter studies of the human gene for the regulatory subunit RII[alpha] of cAMP-dependent protein kinase. Biochim Biophys Acta 1997;1350:98–108.

[29] Diviani D, Soderling J, Scott JD. AKAP-Lbc anchors protein kinase A and nucleates Gα12-selective rho-mediated stress fiber formation. J Biol Chem 2001;276:44247–57.

[30] Chang C-H, Gupta P, Goldenberg DM. Advances and challenges in developing cytokine fusion proteins as improved therapeutics. Expert Opin Drug Discov 2009;4:181–94.

[31] Goldenberg DM, Rossi EA, Sharkey RM, McBride WJ, Chang C- H. Multifunctional antibodies by the Dock-and-Lock method for improved cancer imaging and therapy by pretargeting. J Nucl Med 2008;49:158–63.

[32] Chang C-H, Rossi EA, Goldenberg DM. The dock and lock method: a novel platform technology for building multivalent, multifunctional structures of defined composition with retained bioactivity. Clin Cancer Res 2007;13: 5586s–91s.

[33] Chang C-H, Rossi EA, Cardillo TM, Nordstrom DL, McBride WJ, Goldenberg DM. A new method to produce monoPEGylated dimeric cytokines shown with human interferon-α2b. Bioconjug Chem 2009;20:1899–907.

[34] Studier FW. Protein production by auto-induction in high density shaking cultures. Protein Expr Purif 2005;41:207–34.

[35] Rughani RV, Salick DA, Lamm MS, Yucel T, Pochan DJ, Schneider JP. Folding, self-assembly, and bulk material properties of a de novo designed three-stranded β-sheet hydrogel. Biomacromolecules 2009;10:1295–304.

[36] Yamaguchi N, Zhang L, Chae B-S, Palla CS, Furst EM, Kiick KL. Growth factor mediated assembly of cell receptor-responsive hydrogels. J Am Chem Soc 2007;129:3040–1.

[37] Nowak AP, Breedveld V, Pakstis L, Ozbas B, Pine DJ, Pochan D, et al. Rapidly recovering hydrogel scaffolds from self-assembling diblock copolypeptide amphiphiles. Nature 2002;417:424–8.

[38] Teles H, Skrzeszewska PJ, Werten MWT, van der Gucht J, Eggink G, de Wolf FA. Influence of molecular size on gel-forming properties of telechelic collagen-inspired polymers. Soft Matter 2010;6:4681–7.

[39] Shen W, Zhang K, Kornfield JA, Tirrell DA. Tuning the erosion rate of artificial protein hydrogels through control of network topology. Nat Mater 2006;5: 153–8.

[40] Anderson BC, Pandit NK, Mallapragada SK. Understanding drug release from poly(ethylene oxide)-b-poly(propylene oxide)-b-poly(ethylene oxide) gels. J Control Release 2001;70:157–67.

[41] Lee KY, Mooney DJ. Hydrogels for tissue engineering. Chem Rev 2001;101: 1869–79.

[42] Li J, Ni X, Leong KW. Injectable drug-delivery systems based on supramolecular hydrogels formed by poly(ethylene oxide)s and α-cyclodextrin. J Biomed Mater Res A 2003;65:196–202.

[43] Wheeldon IR, Calabrese Barton S, Banta S. Bioactive Proteinaceous Hydrogels from designed bifunctional building blocks. Biomacromolecules 2007;8:2990–4.

[44] Engler AJ, Sen S, Sweeney HL, Discher DE. Matrix elasticity directs stem cell lineage specification. Cell 2006;126:677–89.